

# Direct Synthesis of Al–SBA-15 Mesoporous Materials via Hydrolysis-Controlled Approach

Ying Li, Wenhua Zhang, Lei Zhang, Qihua Yang, Zhaobin Wei, Zhaochi Feng, and Can Li\*

State Key Laboratory of Catalysis, Dalian Institute of Chemical Physics, Chinese Academy of Sciences, 457 Zhongshan Road, Dalian 116023, China

Received: January 13, 2004; In Final Form: April 22, 2004

Aluminum-substituted mesoporous SBA-15 (Al–SBA-15) materials were directly synthesized by a hydrolysis-controlled approach in which the hydrolysis of the silicon precursor (tetraethyl orthosilicate, TEOS) is accelerated by fluoride or by using tetramethyl orthosilicate (TMOS) as silicon precursor rather than TEOS. These materials were characterized by powder X-ray diffraction (XRD),  $N_2$  sorption isotherms, TEM,  $^{27}\text{Al}$  MAS NMR, IR spectra of pyridine adsorption, and  $\text{NH}_3$ -TPD. It is found that the matched hydrolysis and condensation rates of silicon and aluminum precursors are important factors to achieve highly ordered mesoporous materials.  $^{27}\text{Al}$  MAS NMR spectra of Al–SBA-15 show that all aluminum species were incorporated into the silica framework for the samples prepared with the addition of fluoride. A two-step approach (sol–gel reaction at low pH followed by crystallization at high pH) was also employed for the synthesis of Al–SBA-15. Studies show that the two-step approach could efficiently avoid the leaching of aluminum from the framework of the material. The calcined Al–SBA-15 materials show highly ordered hexagonal mesostructure and have both Brønsted and Lewis acid sites with medium acidity.

## 1. Introduction

The discovery of silica-based and metal-substituted mesoporous materials M41S (MCM-41, MCM-48, MCM-50) has attracted intense interest due to their high surface area, uniform pore size distribution, large pore size, and highly valuable potential applications in the field of catalysis, separation, and adsorption.<sup>1–3</sup> In the family of mesoporous materials, SBA-15 materials synthesized with triblock copolymer as surfactant under strong acidic conditions exhibit larger pore sizes and thicker pore walls compared with M41S. The improved hydrothermal and thermal stability make them some of the most promising catalytic materials.<sup>4</sup> However, it is very difficult to introduce the metal ions into SBA-15 directly due to the facile dissociation of metal–O–Si bonds under strong acidic hydrothermal conditions. Therefore, only a few papers reported the direct synthesis of metal-substituted SBA-15 materials.<sup>5–8</sup> Most work was focused on the postsynthesis method.<sup>9–11</sup> Nevertheless, the postsynthesis method always leads to the extra-framework species and irregularly distributed active sites.<sup>12</sup>

Among the metal-substituted mesoporous materials, aluminum-incorporated mesoporous materials have great potentials in moderate acid-catalyzed reactions for large molecules.<sup>13–15</sup> Yue and co-workers<sup>5</sup> have directly incorporated aluminum into the framework of SBA-15 materials by using tetraethyl orthosilicate (TEOS) and aluminum tri-*tert*-butoxide as silicon and aluminum precursors, respectively. However, the resulting materials have many extra-framework aluminum species. Xiao and co-workers<sup>8</sup> have recently reported a “pH-adjusting” method to graft Al and Ti atoms to SBA-15 materials. It remains a big challenge to directly synthesize Al-substituted SBA-15 materials through a standard hydrothermal method.

The difficulties for the direct synthesis of Al-substituted mesoporous materials under acidic conditions are due to the

too easy dissociation of Al–O–Si bond under acidic hydrothermal condition and the remarkable difference between the hydrolysis rates of silicon and aluminum alkoxides.<sup>16</sup> Several strategies have been used to solve the problems caused by the difference in reactivity toward hydrolysis and condensation of silicon and aluminum alkoxides. Among the strategies are the following: prehydrolysis of the alkoxy-silanes before addition of Al alkoxide;<sup>17</sup> making the mixed metaloxane Si–O–Al bonds at the stage of the precursors;<sup>18</sup> decreasing the hydrolysis rate of aluminum precursors by complexing them with chelating agents such as ethyl acetoacetate.<sup>19</sup> The problem could be also solved by adding some catalysts such as fluoride to accelerate the hydrolysis rates of the silicon precursor<sup>6</sup> or by using precursors with proper alkoxy groups. In our previous work, Ti-substituted SBA-15 materials were successfully synthesized by using fluoride to accelerate the hydrolysis rate of tetramethyl orthosilicate (TMOS) to match that of titanium isopropoxide.<sup>6</sup> However, as far as we know, there has been no report on the synthesis of Al-substituted SBA-15 mesoporous materials by this strategy until now.

In this study, aluminum isopropoxide was used as the aluminum source, which hydrolyzes rapidly to monomeric  $\text{Al}(\text{OH})_4^-$  under acidic or basic conditions. Thus, under the high acidic condition, aluminum isopropoxide was transformed into soluble tetrahedral coordinated Al precursor species that favor the incorporation of tetrahedral Al into the mesoporous materials.<sup>20,21</sup>

The hydrolysis of aluminum isopropoxide is much faster than tetraethyl orthosilicate (TEOS). TMOS hydrolyzes faster than TEOS does, due to the steric hindrance at ethoxide moieties and reduced salvation of resulting ethanol.<sup>22</sup> Therefore, in the present investigation the hydrolysis rates were adjusted by two ways, i.e., by using fluoride as a catalyst to accelerate the hydrolysis rate of TEOS or by using TMOS instead of TEOS as silicon precursor. Furthermore, the pH value of the synthesis solution adjusted by a two-step method efficiently avoids the

\* To whom correspondence should be addressed. Fax: +86-411-84694447. Telephone: +86-411-84379070. E-mail: canli@dicp.ac.cn. Home page: <http://www.canli.dicp.ac.cn>.

leaching of the framework aluminum under acidic condition. Our results demonstrate that both approaches can yield high quality mesoporous Al-SBA-15 materials. The mesoporous Al-SBA-15 materials have moderate acidity and are potential catalysts for many catalytic reactions that do not require strong acid sites, especially for Friedel-Crafts alkylation and acylation reactions involving large molecules.<sup>12,14,23</sup>

## 2. Experimental Section

**Synthesis of Al-SBA-15.** Al-SBA-15 materials were synthesized using tetramethyl orthosilicate (TMOS) or tetraethyl orthosilicate (TEOS) and aluminum isopropoxide (Acros) as silica and aluminum precursors, respectively. Nonionic triblock copolymer surfactant EO<sub>20</sub>PO<sub>70</sub>EO<sub>20</sub> (P123, Aldrich) was used as the structure-directing agent. Concentrated HCl aqueous solution was used as the acid source. NH<sub>3</sub>·H<sub>2</sub>O (25% in mass ratio) was used to adjust the acidity.

**Method 1.** The typical preparation procedure of Al-SBA-15 materials is described as follows: 2 g of P123 and 0.025 g of NH<sub>4</sub>F were dissolved in 75 mL of HCl solution with different pH value to get solution A. Then, 4.6 mL of TEOS (or 3.2 mL of TMOS) and a certain amount of aluminum isopropoxide (Si/Al = 10, 20, 50, 100 in molar ratio) were added to 5 mL of HCl aqueous solution at pH = 1.5 to get solution B. Solution B was stirred at room temperature for about 0.5–3 h, and then it was added dropwise to solution A. The mixture of solution A and B was stirred vigorously for 20 h at 40 °C. Then it was transferred into an autoclave to age for 24 h at 100 °C. The resultant solid was filtered, washed, and dried at 60 °C for 15 h. After the solid was calcined at 500 °C for 10 h, the mesoporous Al-SBA-15 samples were finally obtained.

**Method 2.** Solution A (pH = 1.5) and solution B (a mixture of 0.21 g of aluminum isopropoxide and 3.2 mL of TMOS) were mixed as described in method 1. After the white precipitate appeared (about 10–15 min after solution B was added), a small amount of NH<sub>3</sub>·H<sub>2</sub>O was added drop by drop to adjust the pH value equal to 7.0. The remaining steps were the same as method 1.

**Synthesis of Al-MCM-41.** Na-Al-MCM-41 was synthesized using CTAB as a structure-directing agent according to ref 24 with some modifications; otherwise, a prehydrolysis solution of 25 mL of TEOS and 1.14 g of aluminum isopropoxide instead of TEOS was used. The Na-Al-MCM-41 was refluxed with 1 M NH<sub>4</sub>Cl solution at 80 °C for 6 h to obtain NH<sub>4</sub>-Al-MCM-41, which was further calcined to obtain H-Al-MCM-41.

**Characterizations.** XRD patterns were recorded on a Rigaku D/MAX 3400 powder diffraction system using Cu K $\alpha$  radiation (40 kV and 30 mA) over the range  $0.5 \leq 2\theta \leq 10^\circ$ .

The nitrogen sorption experiments were performed at 77 K on ASAP 2000 system in static measurement mode. The samples were outgassed at 300 °C for 10 h before the measurement. The pore size distribution curves were obtained from the analysis of the desorption branch of the isotherm by the BJH (Barrett-Joyner-Halenda) method.

Transmission electron microscopy (TEM) measurements were taken on a JEM-3010 electron microscope (JEOL Japan) with an acceleration voltage of 300 kV.

<sup>27</sup>Al MAS NMR spectra were recorded at 104.3 MHz on a Bruker DRX-400 spectrometer equipped with a magic angle spin probe at room temperature. AlCl<sub>3</sub>·6H<sub>2</sub>O was used as a reference.

IR spectra of adsorbed pyridine were taken on a Thermo Nicolet NEXUS 470 FT-IR spectrometer. The samples were

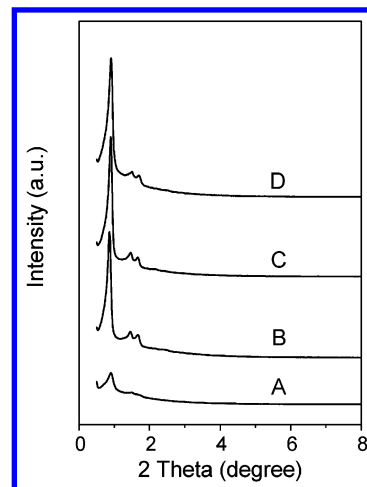


**Figure 1.** Powder XRD patterns of calcined Al-SBA-15 (Si/Al = 20, pH = 1.5): (A) TEOS, without F<sup>-</sup>; (B) TEOS, F<sup>-</sup>/Si = 0.03 (in mol ratio); (C) TMOS, without F<sup>-</sup>; (D) TMOS, F<sup>-</sup>/Si = 0.03 (in mol ratio).

made into self-supporting wafers and were evacuated in an IR cell at 500 °C for 2 h. IR background spectra were recorded after the samples were cooled to room temperature. Pyridine was then admitted into the IR cell and the IR spectra of adsorbed pyridine were recorded after a degassing at 150, 250, and 350, respectively.

NH<sub>3</sub>-TPD measurements were carried out in a flow reactor. Samples were activated at 700 °C for 1 h in a flow of helium; subsequently, ammonia was introduced by a He stream containing 10 (vol) % of ammonia at 100 °C. The physically adsorbed NH<sub>3</sub> was removed by purging with a helium flow at 100 °C until the baseline was flat. Then the reactor temperature was ramped at a rate of 10 °C/min.

## 3. Results and Discussion

**3.1. Effect of Fluoride and Silica Precursors on the Synthesis of Al-SBA-15.** Fluoride is a catalyst for hydrolysis and polymerization of silicon species<sup>24</sup> and has been used in the synthesis of purely siliceous and Ti-substituted mesoporous materials.<sup>6,25–28</sup> Figure 1 shows the XRD patterns of the calcined Al-SBA-15 (Si/Al = 20 in the initial gel, pH = 1.5) samples prepared with TEOS or TMOS as silicon precursors using fluoride as hydrolysis catalyst. For the sample prepared using TEOS as silicon precursor without addition of fluoride (sample A), the XRD pattern shows only one broad *d*<sub>100</sub> peak. For the sample prepared with addition of fluoride (sample B), the XRD pattern shows three well-resolved peaks at (100), (110), and (200) with enhanced intensity. The XRD patterns of the material represent a 2D hexagonal mesostructure with space group *p6mm* with the same structure as mesoporous silica SBA-15.<sup>4</sup> The XRD results show that the structure order of the materials is obviously improved with the addition of fluoride.

When TMOS was used as silicon precursor, well-resolved XRD patterns of typical SBA-15 were obtained for the sample synthesized with fluoride and without fluoride (sample C and sample D). These results suggest that the addition of fluoride has little effect on the structure of materials when a suitable silicon precursor is used.

These phenomena can be explained by the fact that the hydrolysis of aluminum isopropoxide is much faster than TEOS under acidic condition. The addition of fluoride is necessary to accelerate the hydrolysis rates of TEOS when it was used as silicon precursor. Nevertheless, the hydrolysis rate of TMOS

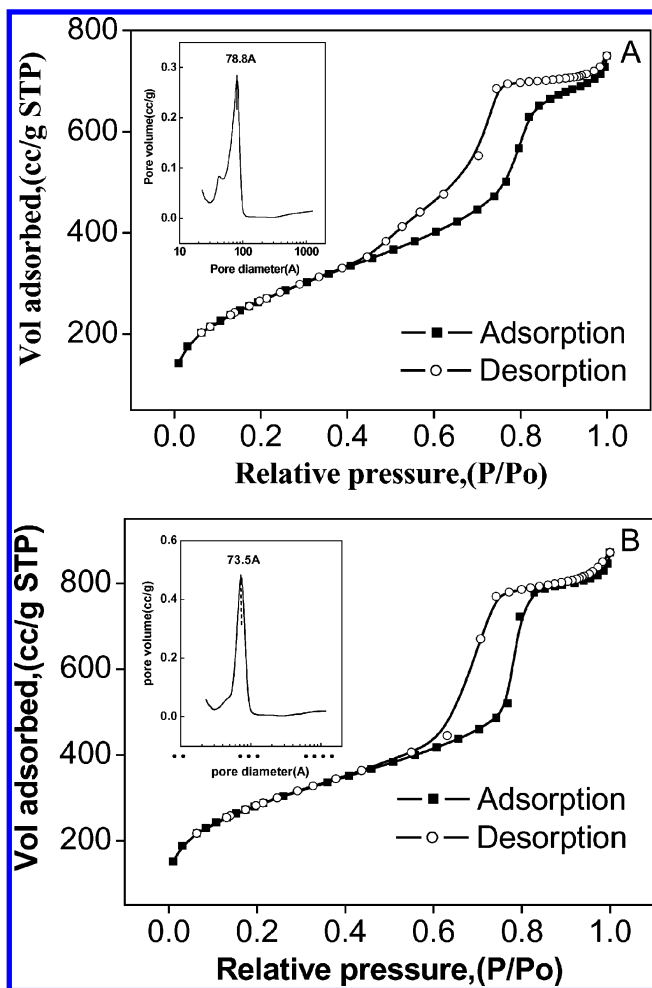


**Figure 2.** Nitrogen adsorption-desorption isotherms and the pore size distributions for calcined Al-SBA-15 (Si/Al = 20, pH = 1.5): (A) TEOS, without F<sup>-</sup>; (B) TEOS, F<sup>-</sup>/Si = 0.03.

is faster than that of TEOS. The hydrolysis rates of TMOS and aluminum isopropoxide may match each other very well. Therefore, the role of fluoride played in the synthesis is not apparent with TMOS as silicon precursor.

The different hydrolysis behaviors of TEOS and TMOS with fluoride and without fluoride were also carefully investigated in this work. During the preparation procedure, when the TMOS was mixed with aluminum isopropoxide and HCl solution, a clear solution was formed in a few minutes. When the same amount of TEOS was mixed with aluminum isopropoxide and HCl solution, the solution was opaque. With addition of fluoride, the precipitation time was shortened significantly from 15 h to 10–20 min using TEOS as silicon precursor. Nevertheless, When TMOS was used as precursor, the precipitate appeared in 5–10 min with fluoride and 10–15 min without fluoride. These facts confirm that the addition of the fluoride can accelerate the rates of hydrolysis and condensation of TEOS, while the hydrolysis and condensation rates of TMOS and aluminum isopropoxide match each other very well.

The porosity of the Al-SBA-15 samples was measured by N<sub>2</sub> sorption. Figure 2 gives the adsorption-desorption isotherms and pore size distributions (inset) of Al-SBA-15 samples prepared by using TEOS as silicon precursor with and without fluoride (Si/Al = 20, the pH value of synthesis solution is 1.5, F<sup>-</sup>/Si = 0.03 in mol ratio). For the sample prepared with fluoride as the catalyst, the isotherm is typical type IV with a H1 hysteresis loop, which is a typical adsorption for mesoporous materials with 2D-hexagonal structure.<sup>4</sup> A well-defined step

**TABLE 1: Texture Properties and Si/Al Ratios of Calcined Al-SBA-15 Materials**

samples	silicon sources	F <sup>-</sup> /Si (in mol ratio)	pH <sup>a</sup>	surface area (m <sup>2</sup> /g)	pore vol (cm <sup>3</sup> /g)	pore diam <sup>b</sup> (nm)	Si/Al in gel	Si/Al <sup>c</sup> in products
A	TEOS	0	1.5	966.2	1.10	7.9	20	28.9
B	TEOS	0.03	1.5	1023.9	1.28	7.4	20	40.5
C	TMOS	0	1.5	965.6	1.17	7.4	20	47.4
D	TMOS	0.03	1.5	922.6	1.29	7.4	20	52.9
E	TEOS	0.03	0	910.2	1.07	7.2	20	<i>e</i>
F	TEOS	0.03	1.0	982.3	1.04	7.4	20	<i>e</i>
G <sup>d</sup>	TEOS	0.03	1.5–7	863.0	1.25	7.4	20	22.0

<sup>a</sup> The pH value refers to the pH value of the initial gel. <sup>b</sup> The pore diameters were calculated by the desorption branch of the isotherms. <sup>c</sup> The Si/Al ratios in the calcined materials were calculated by the ICP-AES method. <sup>d</sup> Sample G was prepared with the two-step method. <sup>e</sup> The Al content is very low, and the sample has no acidity.

occurs at relative high pressure of 0.6–0.8, corresponding to capillary condensation of N<sub>2</sub>, indicative of the uniformity of the pores. Nevertheless, the isotherm of the sample prepared without fluoride shows an obvious hysteresis of the H3 type at  $P/P_0 > 0.8$  as well,<sup>29</sup> corresponding to capillary condensation in the interparticle pores or some impurity phases, which is also shown in XRD patterns. All the samples have surface specific area as large as 900 m<sup>2</sup>/g with the pore volume over 1.1 cm<sup>3</sup>/g and the pore diameters are ca. 7.5 nm (calculated from the desorption branch of the isotherm) (Table 1).

The TEM images of calcined Al-SBA-15 (Si/Al = 20) materials show well-ordered hexagonal arrays of mesopores with one-dimensional channels indicating a 2-D hexagonal (*p6mm*) mesostructure (Figure 3). The distance between two consecutive centers of hexagonal pores estimated from the TEM images is ca. 11 nm. The average thickness of the wall is ca. 4–5 nm, and the pore diameter is around 7–8 nm, in agreement with the N<sub>2</sub> adsorption measurement.

<sup>27</sup>Al MAS NMR spectra of the Al-SBA-15 prepared with TEOS as silicon source are displayed in Figure 4. The spectrum of a sample prepared without fluoride shows two resonance peaks at 0 and 50 ppm. The resonance at 0 ppm can be assigned to octahedral aluminum corresponding to extra-framework aluminum species. The resonance at 50 ppm can be assigned to framework aluminum species in tetrahedral coordination.<sup>30</sup> The sample prepared with addition of fluoride exhibits a single sharp resonance at 50 ppm corresponding to framework aluminum species. This indicates that almost all aluminum atoms are in a tetrahedral environment for the sample prepared with the existence of fluoride. The elemental analysis results indicate that the amount of aluminum in Al-SBA-15 synthesized with fluoride is less than that without fluoride (Table 1). This is because the extra-framework aluminum species are removed by forming the coordination complex with F<sup>-</sup> during the synthesis process.<sup>31,32</sup> However the framework aluminum contents of all the calcined samples are much less than that of the initial gel. The adjustment of the acidity of the synthesis solution may be helpful for increasing the framework aluminum content.

### 3.2. Al-SBA-15 Synthesized by Adjusting the pH Value.

The pH value is an important factor for the synthesis of metal-substituted mesoporous materials. The metal-O-Si bond dissociates easily at high acidity, but high-quality SBA-15 mesoporous materials are difficult to form at low acidity. Figure 5 gives the XRD patterns of the Al-SBA-15 samples prepared with different pH values of HCl aqueous solution before the surfactant P123 was dissolved (Si/Al = 20; F<sup>-</sup>/Si = 0.03; TEOS as silicon source). It should be noted that the pH value increases



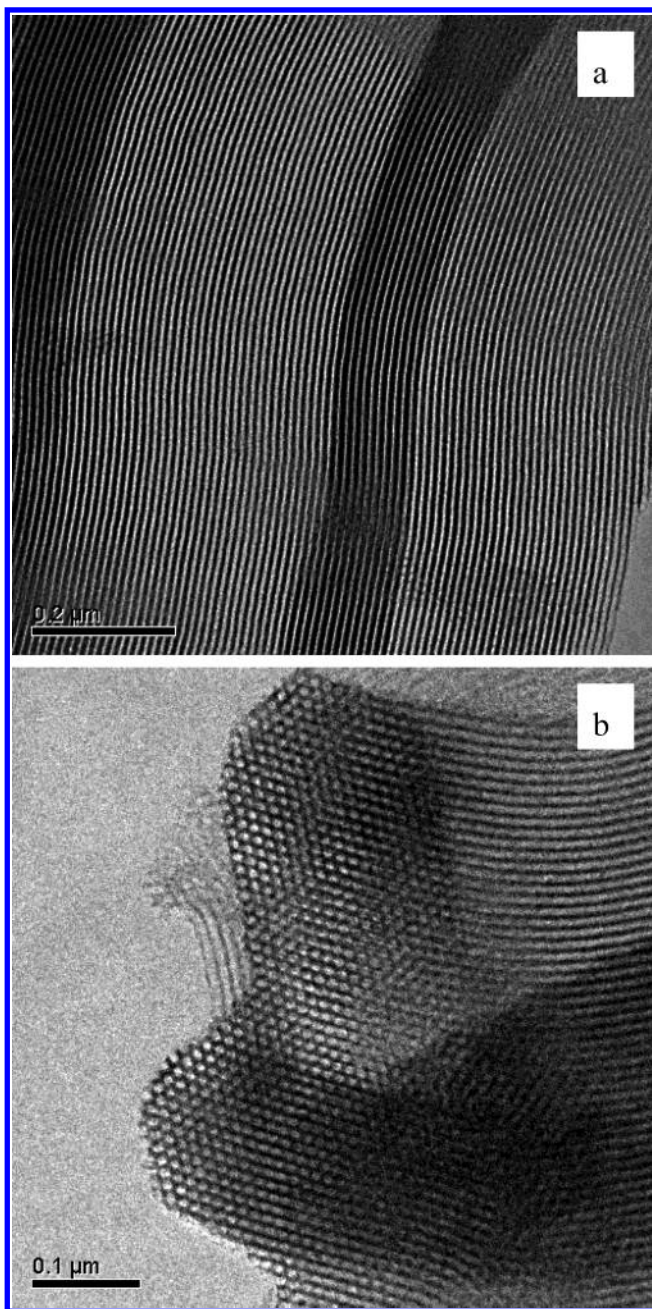


**Figure 3.** TEM images of calcined Al-SBA-15 (Si/Al = 20) (a) in the direction perpendicular to the pore axis and (b) in the direction of the pore axis.

somewhat due to the protonation of the P123 in dilute HCl solution.<sup>4,6,33</sup> All samples prepared at pH value equal to or lower than 1.5 show typical XRD peaks of SBA-15 as reported.<sup>4</sup> However, for the sample prepared at pH = 2.0, only gellike material is formed and the  $d_{100}$  peak is not observed. The isoelectric point of the silica is 2.0. When the pH value is equal to 2.0 in the initial HCl solution, the pH value of the solution is beyond 2.0, so the reaction mechanism between the surfactant p123 and hydrolysis products of silicon and aluminum may change. In fact, for the samples prepared under high acidity conditions (pH  $\leq$  1.0), almost no aluminum species are incorporated into the framework although the resulting materials show highly ordered structures. Therefore, high-quality Al-SBA-15 materials can be only formed at a pH value equal to 1.5 under the present synthesis conditions. The Si/Al ratios in the calcined samples are higher than the Si/Al ratios in the initial gel though the pH value of the synthesis solution was increased

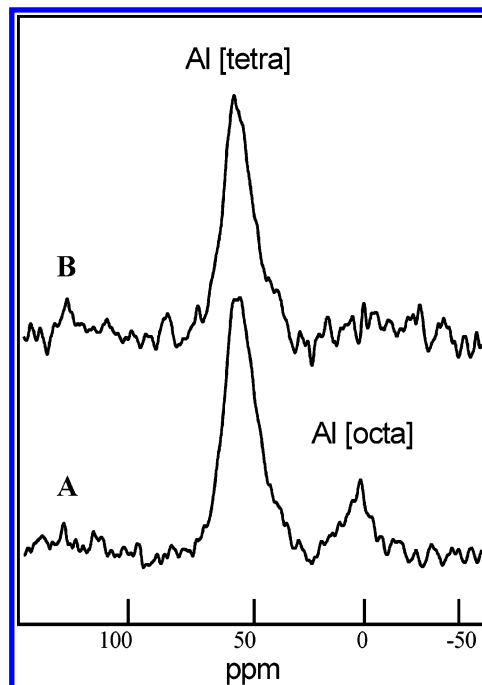


**Figure 4.**  $^{27}\text{Al}$  MAS NMR spectra of calcined Al-SBA-15 (Si/Al = 20, pH = 1.5): (A) TEOS, without  $\text{F}^-$ ; (B) TEOS,  $\text{F}^-/\text{Si} = 0.03$ .

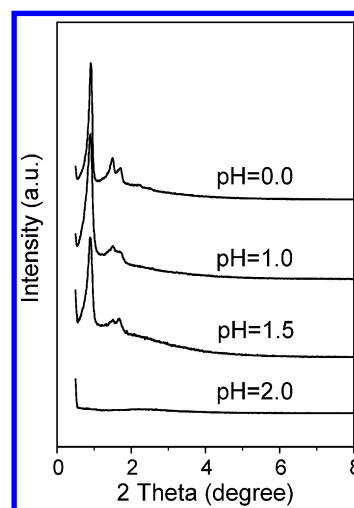


**Figure 5.** Powder XRD patterns of calcined Al-SBA-15 materials (Si/Al = 20, TEOS,  $\text{F}^-/\text{Si} = 0.03$ ) prepared with different pH values.

to 1.5. To solve this problem, we tried to adjust the pH value by a two-step method to decrease the Si/Al ratio.

The two-step sol-gel reaction by abrupt pH change had been used by Yang et al.<sup>34</sup> to synthesize pure silica SBA-15 materials, i.e., a low pH value for the sol-gel reaction followed by a reaction and crystallization at high pH values. Here, we used this method to avoid the leaching of the framework aluminum species from the Al-SBA-15 materials. Ammonium hydroxide was used to induce stepwise pH change in the two-step sol-gel reaction about 10–20 min after the addition of TMOS. Three well-resolved XRD peaks in the XRD pattern (Figure 6) indicate that the structure is not affected by the addition of the  $\text{NH}_3 \cdot \text{H}_2\text{O}$ . It is surprising that the Si/Al ratio can decrease from 40 (sample A) to 22 (sample G, results are given in Table 1) without losing the SBA-15 structure. These results suggest that the pH adjusted by the two-step method is an efficient strategy to avoid the leaching of the framework aluminum from Al-SBA-15. Combined with the results above, it is found that Al-SBA-15

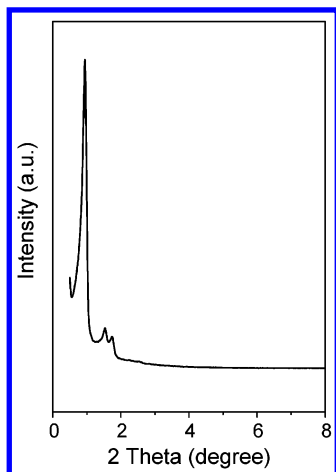


**Figure 6.** Powder XRD patterns of calcined Al-SBA-15 materials (Si/Al = 20, TEOS, F<sup>-</sup>/Si = 0.03) prepared with method 2 (pH adjusted by a two-step method).

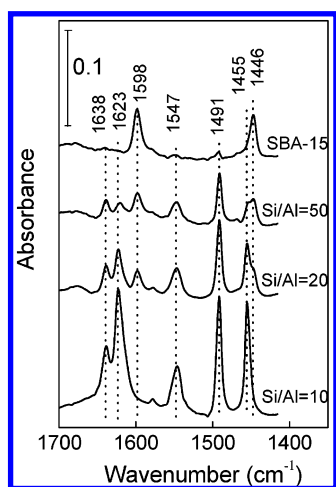


**Figure 7.** IR spectra of pyridine desorbed on Al-SBA-15 with different Si/Al ratios at 150 °C.

materials with high concentrations of framework aluminum can be successfully synthesized through a fine adjustment of the pH value.

**3.3. Acidity of Al-SBA-15 Materials. 3.3.1. IR Spectra of Adsorbed Pyridine.** To evaluate the strength and types of acid sites of Al-SBA-15, pyridine adsorption measured by IR spectroscopy was used. Figure 7 shows the spectra of pyridine desorbed on Al-SBA-15 at 150 °C in the range 1700–1400 cm<sup>-1</sup> for samples with different Si/Al ratios. All the samples with different Si/Al ratios give the IR bands due to hydrogen-bonded pyridine (1447 and 1599 cm<sup>-1</sup>), pyridine adsorbed on Lewis acid sites (1455 and 1623 cm<sup>-1</sup>), pyridine adsorbed on Brönsted acid sites (1547 and 1640 cm<sup>-1</sup>), and a band at 1490 cm<sup>-1</sup> attributed to pyridine associated with both Lewis and Brönsted acid sites.<sup>35</sup> The intensity of the bands at 1455 and 1547 cm<sup>-1</sup> due to Lewis and Brönsted acid sites increases with decreasing Si/Al ratios. This indicates that the acidity increases with decreasing Si/Al ratios. It is interesting to note that as the Si/Al ratios increase, the relative intensity of the band due to weakly held hydrogen-bonded pyridine increases compared to the other characteristic bands.<sup>36</sup> The IR spectrum of pyridine adsorption on pure silica SBA-15 material shows no peaks at 1455 or 1547 cm<sup>-1</sup> attributed to Lewis or Brönsted acid sites, respectively.

The IR spectra of adsorbed pyridine on the samples after evacuation at 150, 250, and 350 °C were taken in order to

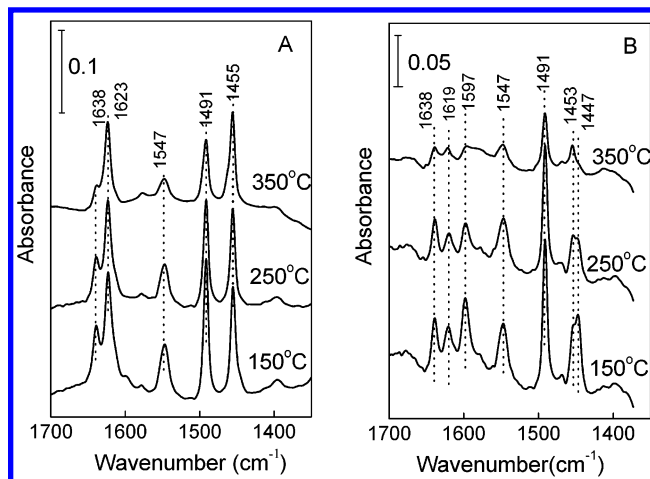


**Figure 8.** IR spectra of pyridine desorbed on calcined Al-SBA-15 materials (Si/Al = 20) at 150, 250, and 350 °C: (A) TEOS, without F<sup>-</sup>; (B) TEOS, F<sup>-</sup>/Si = 0.03.

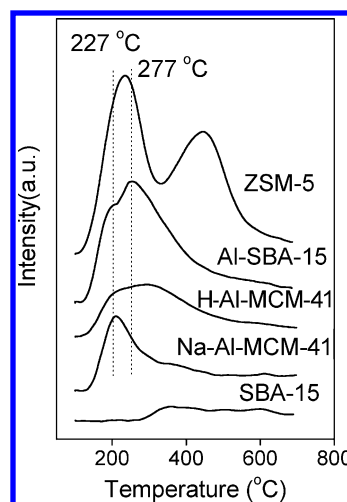


**Figure 9.** NH<sub>3</sub>-TPD profiles of Al-SBA-15 (Si/Al = 10), SBA-15, Na(H)-Al-MCM-41 (Si/Al = 10), and ZSM-5 (Si/Al = 50).

estimate the strength of the acidity. Figure 8 shows the IR spectra of pyridine adsorbed on Al-SBA-15 synthesized with or without fluoride using TEOS as silicon precursor. The intensity ratio of the band at 1547 cm<sup>-1</sup> (Brönsted acid site) to that at 1455 cm<sup>-1</sup> (Lewis acid site) is smaller for the sample prepared without fluoride (Figure 8A) compared with the sample with fluoride (Figure 8B). This is consistent with the <sup>27</sup>Al NMR results, as the Brönsted acid sites are mainly originated from the framework aluminum species. However, the total amount of acidic sites of the sample prepared with fluoride is less than that of the sample without fluoride due to the difference in the Si/Al ratios in the calcined samples. When the desorption temperature is increased to 350 °C, the band at 1547 cm<sup>-1</sup> due to pyridine adsorbed on Brönsted acid sites and the band at 1455 cm<sup>-1</sup> on Lewis acid sites still exist. This clearly indicates that the acidity of Al-SBA-15 is quite strong.

**3.3.2. NH<sub>3</sub>-TPD.** Figure 9 shows the NH<sub>3</sub>-TPD profiles of Al-SBA-15 (Si/Al = 10), SBA-15, Na(H)-Al-MCM-41 (Si/Al = 10), and ZSM-5 (Si/Al = 50). The TPD profile of ZSM-5 shows two typical peaks at 245 and 460 °C, which correspond to weak and strong acidic sites, respectively. The TPD profile of pure silica SBA-15 material shows no evident peaks, indicating that SBA-15 material has no acid sites. The TPD profile of calcined Na-Al-MCM-41 shows only one peak at 227 °C, while the TPD profile of H-Al-MCM-41 shows an

extra peak at 277 °C as well. These results indicate that the peak at 277 °C may be corresponding to the desorption of NH<sub>3</sub> from the medium acid sites of the materials and the peak at 227 °C may be corresponding to the desorption of NH<sub>3</sub> from the weak acid sites of the materials. The TPD profile of Al-SBA-15 shows a sharp peak at 277 °C and a shoulder peak at 227 °C. The sharp peak at 277 °C indicates that Al-SBA-15 materials are abundant with medium acid sites.

The peak at 277 °C in the TPD profile of Al-SBA-15 is much sharper than that of H-Al-MCM-41 and the total peak area is larger than that of H-Al-MCM-41, indicating that Al-SBA-15 materials have more medium acidic sites than that of Al-MCM-41 with same Si/Al ratios. However, the acidity of Al-SBA-15 and Al-MCM-41 is still weaker than that of ZSM-5, due to the amorphous nature of the pore wall of the mesoporous materials.

#### 4. Conclusions

The highly ordered mesoporous Al-substituted SBA-15 materials have been directly synthesized by a hydrolysis-controlled method. The hydrolysis and condensation rates of silicon and aluminum precursors were finely controlled to match each other by using fluoride or by using TMOS rather than TEOS. All aluminum species were incorporated into the silica framework for the samples prepared with the addition of fluoride. The pH value of the synthesis solution adjusted by a two-step method efficiently avoids the leaching of the aluminum species from the Al-SBA-15 under acidic conditions. In summary, the matched hydrolysis and condensation rates of silicon and aluminum precursors are important factors to achieve highly ordered mesoporous materials. Moreover, the proper adjustment of the synthesis acidity is also crucial to increase the content of framework aluminum in Al-SBA-15. Pyridine adsorption results show that the Al-SBA-15 materials have both Lewis and Brønsted acid sites. The Al-SBA-15 materials have moderate acidity according to the NH<sub>3</sub>-TPD results, and Al-SBA-15 materials have more medium acidic sites than that of Al-MCM-41 with the same Si/Al ratios.

**Acknowledgment.** This work was financially supported by the National Basic Research Program of China (Grant Nos. G2000048003, G1999022407, 2003CB615806, 2003CB615803). The authors would like to thank to Prof. F. S. Xiao of Jilin University in China for the TEM measurement of the samples and the helpful discussions.

#### References and Notes

- (1) Kresge, J. S.; Leonowicz, M. E.; Roth, W. J.; Vartuli, J. C.; Beck, J. S. *Nature (London)* **1992**, 359, 710. (b) Beck, J. S.; Vartuli, J. C.; Roth, W. J.; Leonowicz, M. E.; Kresge, C. T.; Schmitt, K. D.; Chu, C. T. W.; Olson, D. H.; Sheppard, E. W.; Cullen, S. C.; Higgins, J. B.; Schlenker, J. L. *J. Am. Chem. Soc.* **1992**, 114, 10834.
- (2) Corma, A.; Grand, M. S.; Gonzalez, A. V.; Orichilles, A. V. *J. Catal.* **1996**, 159, 375.
- (3) Selvaraj, M.; Pandurangan, A.; Seshadri, K. S.; Sinha, P. K.; Krishnasamy, V.; Lal, K. B. *J. Mol. Catal. A: Chem.* **2002**, 186, 173. (b) Jana, S. K.; Takahashi, H.; Nakamura, M.; Kaneko, M.; Nishida, R.; Shimizu, H.; Kugita, T.; Namba, S. *Appl. Catal., A: Gen.* **2003**, 245, 33.
- (4) Zhao, D.; Feng, J.; Huo, Q.; Melosh, N.; Fredrickson, G. H.; Chmelka, B. F.; Stucky, G. D. *Science (Washington, D.C.)* **1998**, 279, 548. (b) Zhao, D.; Huo, Q.; Feng, J.; Chmelka, B. F.; Stucky, G. D. *J. Am. Chem. Soc.* **1998**, 120, 6024.
- (5) Yue, Y.; Cedeon, A.; Bonardet, J. L.; Melosh, N.; D'Esinose, J. B.; Fraissard, J. *Chem. Commun.* **1999**, 1967. (b) Cedeon, A.; Lassoued, A.; Bonardet, J. L.; Fraissard, J. *Micro. Meso. Mater.* **2001**, 44–45, 801.
- (6) Zhang, W. H.; Lu, J.; Han, B.; Li, M.; Xiu, J.; Ying, P.; Li, C. *Chem. Mater.* **2002**, 14, 3413.
- (7) Newalkar, B. L.; Olanrewaju, J.; Komarneni, S. *Chem. Mater.* **2001**, 13, 552.
- (8) Wu, S.; Han, Y.; Zou, Y. C.; Song, J. W.; Zhao, L.; Di, Y.; Liu, S. Z.; Xiao, F. S. *Chem. Mater.* **2004**, 16, 486.
- (9) Morey, M. S.; O'Brien, S.; Sch Warz, S.; Stucky, G. D. *Chem. Mater.* **2000**, 12, 898.
- (10) Cheng, M. J.; Wang, Z.; Sakurai, K.; Kumata, F.; Saito, T.; Komatsu, T.; Yashima, T. *Chem. Lett.* **1999**, 131.
- (11) (a) Luan, Z.; Hartmann, M.; Zhao, D.; Zhou, W.; Kevan, L. *Chem. Mater.* **1999**, 11, 1621. (b) Sumiya, S.; Oumi, Y.; Uozumi, T.; Sano, T. *J. Mater. Chem.* **2001**, 11, 1111.
- (12) (a) Murugavel, R.; Roesky, H. W. *Angew. Chem., Int. Ed.* **1997**, 109, 4491. (b) Han, Y.; Meng, X.; Guan, H.; Yu, Y.; Zhao, L.; Xu, X.; Yang, X.; Wu, S.; Li, N.; Xiao, F. *Micro. Meso. Mater.* **2003**, 57, 191.
- (13) Armengol, E.; Cano, M.; Corma, A.; Garcia, H.; Navaro, M. J. *Chem. Soc., Chem. Commun.* **1995**, 519.
- (14) Makaya, R.; Jones, W. J. *Catal.* **1997**, 172, 211.
- (15) Pauly, J. R.; Liu, Y.; Pinnavaia, T. J.; Brillinger, S. J. L.; Rieker, T. P. *J. Am. Chem. Soc.* **1999**, 121, 8835.
- (16) Hernatedez, C.; Pierre, A. C. *Langmuir* **2000**, 16, 530.
- (17) Yoldas, B. E.; Partlow, D. P. *J. Mater. Sci.* **1998**, 23, 1895.
- (18) Lopez, T.; Asmoza, M.; Gomez, R. *J. Non-Cryst. Solids* **1992**, 147&148, 769.
- (19) Pierre, A. C.; Elaloui, E.; Pajonk, G. M. *Langmuir* **1998**, 14, 66.
- (20) Turova, N. Y.; Kozunov, V. A.; Yanovskii, A. I.; Bokii, N. G.; Struchkov, Y. T.; Tarnopolskii, B. L. *J. Inorg. Nucl. Chem.* **1979**, 41, 5. Akitt, J. W.; Duncan, R. H. *J. Magn. Reson.* **1974**, 15, 162.
- (21) Janicke, M. T.; Landry, C. C.; Christiansen, S. C.; Birtalan, S.; Stucky, G. D.; Chmelka, B. F. *Chem. Mater.* **1999**, 11, 1342.
- (22) Brinker, C. J.; Scherer, G. W. *Sol-Gel Science*; Academic Press: London, 1990; pp 97–234. (b) Brinker, C. J. *J. Non-Cryst. Solids* **1988**, 100, 31.
- (23) Chiu, J. J.; Pine, D. J.; Bishop, S. T.; Chmelka, B. F. *J. Catal.* **2004**, 221, 400.
- (24) Zhang, W.; Shi, J.; Chen, H.; Hua, Z.; Yan, D. *Chem. Mater.* **2001**, 13, 648.
- (25) (a) Prouzet, E.; Pinnavaia, T. J. *Angew. Chem., Int. Ed. Engl.* **1997**, 36, 516. (b) Silva, F. H. P.; Pastore, H. Q. *Chem. Commun.* **1996**, 833. (c) Voegtlin, A. C.; Ruch, F.; Guth, J. L.; Patarin, J.; Huve, L. *Micro. Mater.* **1997**, 9, 95. (d) Boissière, C.; Larbot, A.; Van der Lee, A.; Prouzet, E. *Chem. Mater.* **2000**, 12, 2902. (e) Boissière, C.; Larbot, A.; Prouzet, E. *Chem. Mater.* **2000**, 12, 1973.
- (26) Feng, P.; Xia, Y.; Feng, J.; Bu, X.; Stucky, G. D. *Chem. Commun.* **1997**, 949.
- (27) Kim, J. M.; Han, Y. J.; Chmelka, B. F.; Stucky, G. D. *Chem. Commun.* **2000**, 2437.
- (28) Schmidt, W. P.; Yang, P.; Margolese, D. I.; Chmelka, B. F.; Stucky, G. D. *Adv. Mater.* **1999**, 11, 303.
- (29) Sing, K. S. W.; Everett, D. H.; Haul, R. A. W.; Moscou, L.; Pierotti, R. A.; Ronquerol, J.; Siemieniowska, T. *Pure Appl. Chem.* **1985**, 57, 603.
- (30) Xu, M.; Wang, W.; Seiler, M.; Buchholz, A.; Hunger, M. *J. Phys. Chem. B* **2002**, 106, 3202.
- (31) Impe'ror-Clerc, M.; Davidson, P.; Davidson, A. *J. Am. Chem. Soc.* **2000**, 122, 11925.
- (32) Chakraborty, B.; Viswanathan, B. *Catal. Today* **1999**, 19, 253.
- (33) Morterra, C.; Cerrato, G. L. *Langmuir* **1990**, 6, 1810.
- (34) Choi, D. G.; Yang, S. M. *J. Colloid Interface Sci.* **2003**, 261, 127.
- (35) (a) Parriss, E. P. *J. Catal.* **1963**, 2, 371. (b) Emeis, C. A. *J. Catal.* **1993**, 141, 347.
- (36) Valyon, J.; Lonyi, F. *Micro. Meso. Mater.* **2001**, 47, 293.